Paper No.
7664

NACE INTERNATIONAL CORROSION 2016 CONFERENCE & EXPO

Study and Modeling of the Localized Nature of Top of the Line Corrosion

Singer, Marc
Ohio University - ICMT
342 West State St., Athens, OHIO, 45701

ABSTRACT

The occurrence of localized corrosion in Top of the Line Corrosion (TLC) was investigated in a sweet (CO_2-dominated) environment, with a focus on understanding the influence of the environmental parameters on localized TLC in order to develop a narrative for the mechanism.

A unique setup was developed for the experimental work, involving the use of carbon steel inserts exposed to three different levels of cooling at the same time. This concept was quite successful in simulating realistic localized features. A series of long term exposure (one- to three-month) experiments was conducted to investigate the controlling parameters. The occurrence of localized corrosion could be very clearly correlated to the condensation rate, the gas temperature and the organic acid content. Additional statistical information related to the morphology of localized TLC features could be made, providing useful insight on the mechanisms involved.

INTRODUCTION

When significant heat exchange is present between the wet gas pipelines and the surroundings (frozen land, deep-sea water, etc.), water and hydrocarbon vapor can condense on the inner pipe wall and lead to severe corrosion issues [1]. This phenomenon called Top of the line corrosion (TLC) is inherently a localized process. Corrosion occurs in specific areas along the line and the attack is not usually extended to large sections. This localized aspect is often related to situations where high condensation rates occur, *i.e.* where the gradient of temperature between the produced fluid and the outside environment is large. In sweet environments (CO_2-dominated), the corrosion process is often characterized as a mesa attack: the steel is not uniformly corroded but the pits are usually wide, often flat-bottomed and bare of any layers, surrounded by areas with intact corrosion product layers.

The localized nature of TLC is still not well understood. The corrosion features observed in the field can be so large that the corrosion process is often referred to as “localized uniform corrosion” instead of a just “localized corrosion”. The unique TLC scenario where droplets of condensed water appear and are

renewed continuously at the metal surface must play a crucial role. It is likely that the condensation process initiates and promotes the localized corrosion at the top of the line by challenging the protectiveness of the iron carbonate layer.

There is a clear need to develop a better understanding of the mechanisms of sweet localized corrosion in order to provide more accurate predictions of the likelihood of occurrence and the severity of the attack. This would have direct implications in pipeline design and operation. To achieve this goal, it is also important to develop the right experimental tools. No laboratory setup can perfectly represent the conditions in the field. While pure corrosion issues have been successfully simulated in small scale set-ups, the flow conditions relative to a 30" ID pipeline are not easily reproducible.

While several different experimental setups have been used with some success at the Institute for Corrosion and Multiphase Technology (ICMT) at Ohio University and elsewhere, it is believed that significant improvements can be made in the way TLC is simulated.

LITERATURE REVIEW

In the past twenty years, TLC has been the subject of intensive research. Olsen et al. [2] conducted a systematic experimental study on parameters influencing TLC in sweet conditions. The formation of a protective $FeCO_3$ corrosion product layer was suggested to play a key role. The precipitation of $FeCO_3$ only occurs when the saturation level is above the value of one. High levels of super-saturation in $FeCO_3$ could lead to very dense and protective $FeCO_3$, as was the case at a high temperature (70°C) and a low condensation rate. The authors also found that the competition between the rate of iron dissolution (*i.e.*, the increase of Fe^{2+} ions in the aqueous phase) and the water condensation rate controlled the extent of $FeCO_3$ film formation. At a high condensation rate, the saturation in $FeCO_3$ is more difficult to obtain due to the rate of fresh water renewal.

In 2000, Pots et al. [3] conducted a series of experiments aimed at highlighting the competition between the scale formation rate linked to the iron dissolution and the condensation rate. Pots developed a corrosion prediction model for TLC based on the calculation of the concentration of iron at saturation under film-forming conditions. The author emphasized the importance of correctly evaluating the condensation rate in order to accurately predict the corrosion rate.

In 2002, Vitse et al. [4] completed a thorough experimental and theoretical study on TLC caused by carbon dioxide. Condensation and corrosion experiments were conducted in a large-scale 4" ID flow loop, which represented a significant improvement on what had been done before. This setup was later upgraded and improved for the purpose of the present study. Vitse was able to link high gas temperatures to larger condensation rates and consequently to corrosion rates at the top of the line. However, Vitse observed that the formation of $FeCO_3$ was favored by high fluid temperature and could lead to a decrease in the corrosion rate. The experiments also explored the effect of the gas velocity and partial pressure of CO_2 on TLC, which play an important role in the water condensation rate and corrosion rate, respectively. However, the experiments conducted by Vitse were all of relatively short duration (2-4 days) and consequently could not capture the full extent of the corrosion, especially in terms of localized corrosion, which often requires weeks of exposure. Nevertheless, Vitse's corrosion model constituted a considerable breakthrough in the understanding of the mechanisms involved in TLC.

Several experimental studies [5-7] have been published on the effect of different parameters such as acetic acid, Mono-Ethylene-Glycol (MEG) or pH control. However, these experiments also had a relatively short exposure time and offered only limited data in terms of localized corrosion. MEG is commonly used in gas fields in order to prevent the formation of methane gas hydrate (a solid ice structure which can obstruct the flow). The presence of a large quantity of MEG (typically 50 to 70 wt%) decreases the water vapor pressure, which effectively inhibits hydrate formation. It also decreases the water condensation since the amount of water vapor is lower. pH control (a method consisting of

injecting a base in order to control the bulk aqueous pH) was shown to have no real effect on TLC other than limiting the concentration of undissociated acetic acid in the bulk liquid phase available for evaporation. The presence of acetic acid was found to greatly affect TLC and mild steel corrosion in general.

Major advances in TLC research were published in 2007. Zhang et al. [8] published the first fully mechanistic approach in TLC modeling, covering the three main processes involved in top of the line corrosion phenomena: dropwise condensation, chemistry in the condensed water and corrosion at the steel surface. Zhang's approach represents one of the most advanced attempts to model the mechanisms involved in TLC to date. It takes into account the most important parameters in CO_2 TLC: condensation rate, gas temperature, CO_2 partial pressure, gas velocity and acetic acid concentration. Zhang actively participated in the collection of some of the experimental data shown in the present study, and these data were used to validate his model.

Singer [5] published the results of this experimental parametric study of sweet TLC (CO_2 dominated) performed in 4"ID flow loops. This study summarized the effect of the most influencing parameters on which the severity of the corrosion attack depends: the condensation rate, the gas temperature, the gas flow rate, the CO_2 partial pressure and the presence of organic acid. Information about both uniform and localized corrosion was collected through this series of long-term experiments (3 weeks long).

In 2011, Rotimi [9] conducted a series of long-term experiments (up to 6 weeks of exposure) in an autoclave especially designed for TLC study. The effect of water condensation and temperature was evaluated under different partial pressures of CO_2. The author reported that the uniform corrosion decreased as the temperature increased, due to the formation of a more protective $FeCO_3$ layer. However, no information was reported on localized corrosion although this type of corrosion was expected to play a big role in these conditions.

Even though much progress has been made over the years in the understanding of TLC mechanisms, none of the models proposed thus far addresses the occurrence and prediction of localized corrosion. The first experimental study focusing on this aspect linked to TLC phenomena was published by Amri [11], in an effort to relate pit growth and environmental conditions. A conceptual model of pit propagation and growth was proposed, although more validation work is clearly needed since the experimental work was not performed in a setup designed to simulate a representative environment.

RESEARCH OBJECTIVES

As mentioned above, since the present understanding of the localized nature of top of the line corrosion is limited, more work needs to be done to identify the controlling mechanisms. The objectives of the current project are stated as follows:

1. Devise new experimental setups and procedures, which can realistically simulate typical top of the line corrosion (in terms of flow, geometry, corrosive environment, condensation regime) as it is observed in the oil and gas field.
2. Investigate the effect of different influencing parameters on top of the line corrosion (both uniform and localized rates), including the effect of the condensation rate, gas temperature and concentration of acetic acid
3. Implement various methods to qualitatively and quantitatively characterize the interaction between condensation pattern and corrosion attack and to define the localized nature of top of the line corrosion processes.

EXPERIMENTAL PROCEDURE

The experimental setup used for this study has been described elsewhere [5, 12] and only original aspects are presented below.

The experiments were carried out in a high-temperature, high-pressure, 4” ID (0.1 m internal diameter) flow loop. The flow loop is comprised of a large tank (1000L) holding the bulk liquid phase, a gas blower (and in some cases a liquid pump), and a system of 4”ID (0.1 m internal diameter) stainless steel pipes forming a loop. The system is about 30 meters in total length. Various monitoring devices (pressure gauge, thermometers, gas flow meter, liquid sampling device) are installed along the pipe system. Several test sections, where the actual corrosion measurements are performed, are located along the pipe system.

The test section utilized for this study was derived from the “flat slab” concept aiming at simulating the large pipe curvature of a 30” ID (0.76 m internal diameter) pipeline -- a size commonly encountered in oil and gas fields – which is much closer to a flat surface than the 4” ID pipe is. A portion of a pipe section was especially manufactured in order to enable the insertion of a thick flat stainless steel slab about 1m long (Figure 1). The stainless steel slab and the pipe were sealed together using a thermally resistant silicon resin. On top of the stainless steel slab lays an aluminum slab containing a cooling system that enabled the control of the condensation rate.

a) b)

Figure 1: Design of the carbon steel insert in stainless steel slab (a) and b))

Three 20 cm long zones with different cooling areas were created (Figure 2): A well-insulated section {1}, a section not insulated but not subject to forced external cooling {2}, and a section subject to high external cooling {3}. Pictures of the actual setup are shown in Figure 2.

A set of thermistors embedded in the stainless steel component was used to monitor the steel temperature and compute the condensation rate on each section. The condensation rate was determined by measuring the difference in temperature between the gas and the pipe wall's inner surface using a model developed by Zhang et al. [8].

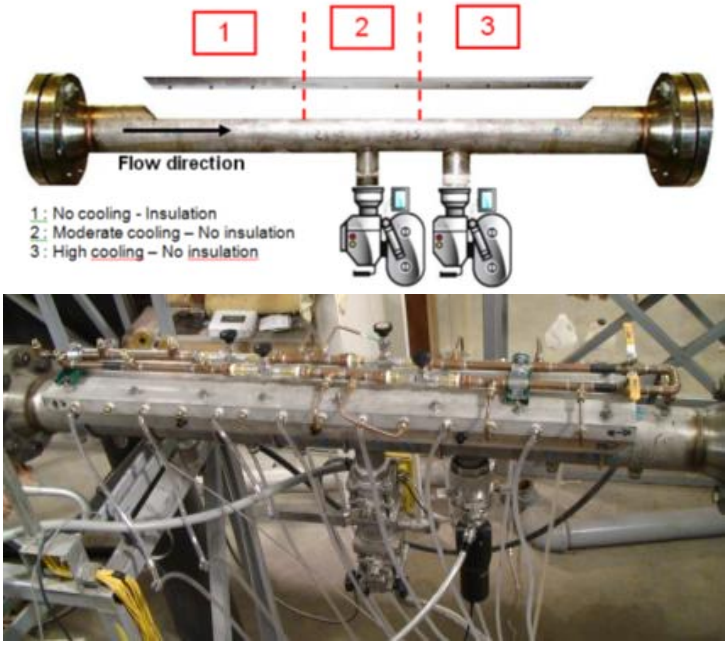

Figure 2: Flat slab cooling setup and stainless steel flat slab equipped with carbon steel insert and aluminum heat exchanger

TEST MATRIX

The test matrix below (Table 1) was selected in order to investigate the effect of the water condensation using an experimental setup designed to simulate the field environment more realistically.

Table 1: Localized condensation/corrosion study - Test matrix
Common parameters:
Test duration: 3 months
Gas velocity: 2.5 m/s - pCO_2= 2.7 bars - pH_2S= 0 bar - P_T= 3 bars

Test #	1	2	3	4
Investigating	Gas temperature			CO_2/HAc
Steel type	C1018(I)	X65	X65	C1018(III)
Tg (°C)	**65**	**45**	**25**	65
Undissociated HAc (ppm)	0	0	0	**1000**
Low WCR (mL/m^2/s)	0.13	0.1	0.04	0.2
Medium WCR (mL/m^2/s)	0.41	0.14	0.06	0.4
High WCR (mL/m^2/s)	0.9	0.22	0.1	0.7

Although steels with different microstructure and composition were used in the study, no difference in corrosion mechanism could be noticed.

EXPERIMENTAL RESULTS

This section presents a summary of the most relevant experimental work performed with the new “flat slab” concept. More details can be found in the original publication [12].

- Influence of the gas temperature and the water condensation rate

TEST #1 - T_{gas}=65°C

The part of the steel insert exposed to a low condensation rate (0.12-0.15 mL/m^2/s) did not seem to be highly corroded (*i.e.*, the corrosion product layer was still fairly intact). The part of the insert exposed to a high condensation rate (0.76-0.95 mL/m^2/s) seemed much more affected by corrosion. Numerous failures of the corrosion product layer (which is usually related to extensive localized corrosion) could be observed, especially on the section exposed to higher water condensation rates. A yellow/orange color could be found on part of the steel sample is a sign of the presence of iron oxide (most likely ferric oxide) which is thought to have formed after the end of the experiment as the slab assembly was removed from the loop. Operational procedures often require a few minutes before the steel insert, wetted by droplets of condensed water saturated with species generated due to corrosion processes, can be accessed and dried. In this elapsed time, the steel is exposed to air. During the experiment itself, great care is given to maintain the level of oxygen in the bulk liquid phase below 20 ppb so as not to interfere with the corrosion process.

The SEM/EDS analysis of the corrosion product layer showed that no significant difference in type and composition was observed with regard to the change in water condensation rates. Although no X-ray diffraction analysis was performed, the corrosion product layer is believed to be a mixture of iron carbonate and iron oxide. Once again, the iron oxide (most likely ferric oxide Fe_2O_3) must have formed

during the removal of the slab assembly at the end of experiment, since no oxygen was present in the loop during the experiment. Some crystals of $FeCO_3$ could be seen underneath the ferric oxide layer.

These initial observations were confirmed with the surface analysis on the bare steel shown in Figure 3 (once the corrosion product layer was removed using Clarke's solution (inhibited HCl)).

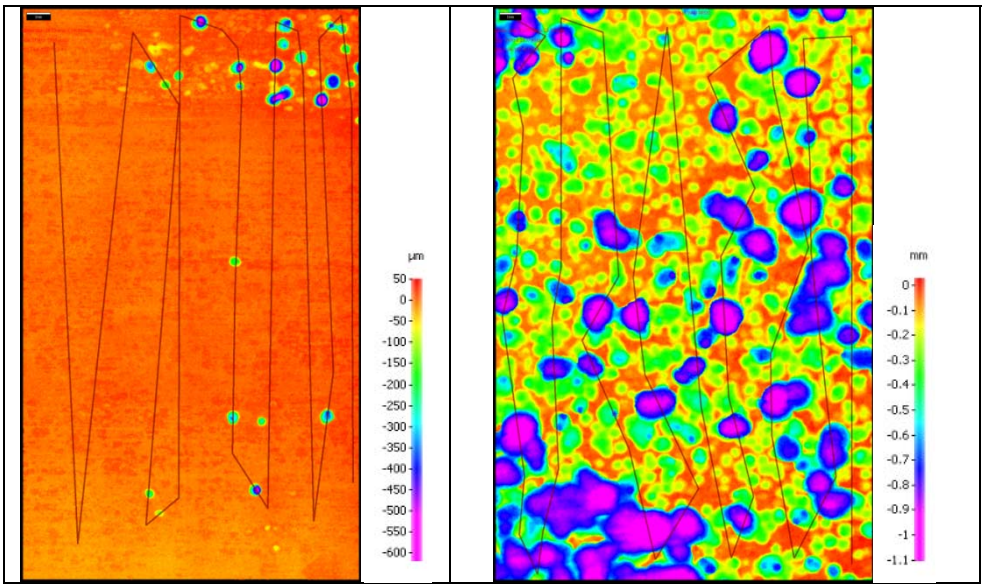

Figure 3: Test #1 - Surface profile analysis after the removal of the corrosion product layer
Left: Upstream section - Low condensation (0.12-0.15 mL/m^2/s)
Right: Downstream section - High condensation (0.76-0.95 mL/m^2/s)

The section of the insert exposed to a low condensation rate did present some pitting corrosion but the pits were fairly isolated. In the middle section exposed to a medium condensation rate (not shown in this publication), the pitting density increased. The pits seemed to coalesce in the section exposed to a high condensation rate which also showed severe mesa attack (localized corrosion with flat bottom features). The relationship between condensation rate and localized corrosion is, therefore, clearly demonstrated in this experiment. These corrosion features very much resemble what is observed in real field situations [1].

Average, minimum and maximum localized corrosion rates were extracted from the 3D profile analysis of selected areas thought to be representative. The localized corrosion data are presented in Figure 4 a) and compared to experimental data obtained under the same conditions but for an exposure time of 21 days [5]. The "21-day" experimental data were obtained by performing a surface profile scan on weight loss samples. Comparing the data obtained after 21 days and 93 days of exposure, the localized corrosion rates (or more accurately – the steel penetration rates) clearly increase with the water condensation rate but also decrease with time. Another way to compare the two sets of data is to plot the actual feature depth versus the condensation rate (Figure 4 b)). It is interesting to note that at condensation rates lower than 0.4 mL/m^2/s, the average feature depth after 21 days and 93 days of exposure is very similar. It could mean that the pit or mesa attack penetration rate significantly slowed down after 21 days of exposure. At a condensation rate of 1 mL/m^2/s, the localized attack depth measured after 93 days of exposure is almost 50% higher than the one measured after 21 days of testing. The hypothesis here is that TLC may have significantly slowed down at a condensation rate below 0.4 mL/m^2/s while it did not at a condensation rate of 1 mL/m^2/s. This is in some ways consistent with field observations noting the existence of a "threshold" water condensation rate in sweet environments below which TLC is not a lasting issue [13]. The maximum feature depths do show the same trend, although the "threshold" water condensation rate seems to be much lower.

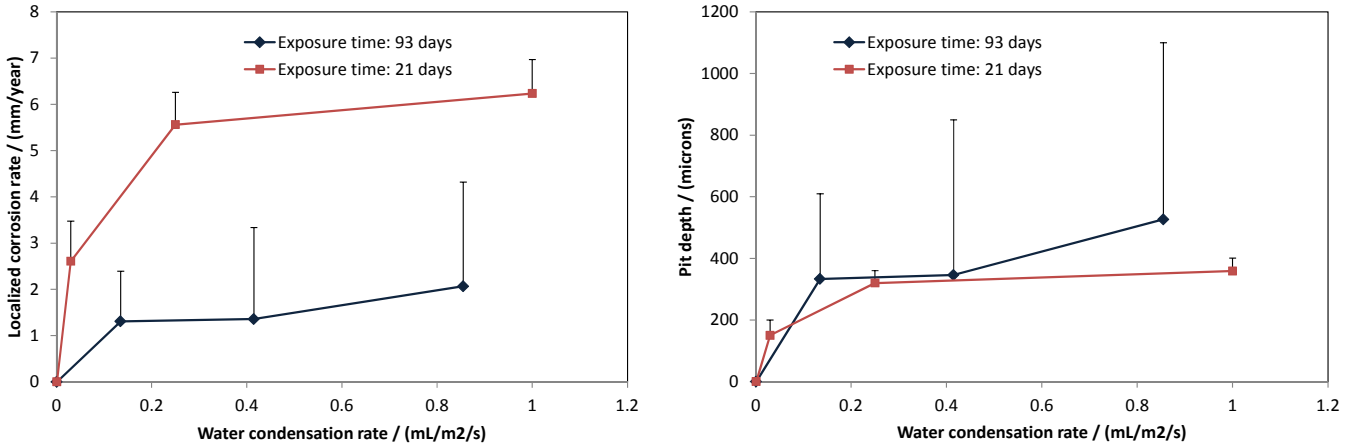

a) b)

Figure 4: Test #1 - a) Influence of the condensation rate on the localized corrosion rate b) Influence of the condensation rate and the exposure time on the pit/mesa depth

The percentage area affected by localized corrosion could also be measured on the steel and the results are displayed in Figure 5 and compared with data obtained for 21 days of exposure. It is clear that, with time, a higher proportion of the steel surface area is corroded when the water condensation rate is high. This is again in agreement with field observations which seem to show that, although TLC corrosion features depth may not progress at a fixed rate, their numbers do increase with time [10]. As the features grow in number, they coalesce and the steel surface becomes more uniformly attacked. This is clearly demonstrated by the data collected in Figure 3, which shows the number of pits per surface area increasing with condensation rate, together with the average feature diameter. The maximum depth of the feature does increase as well, but to a lesser extent.

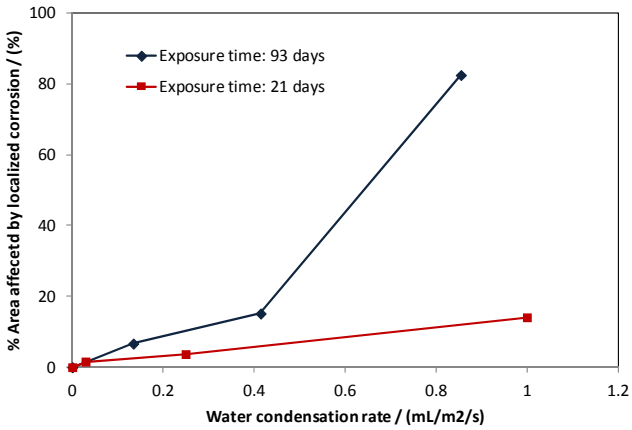

Figure 5: Test #1 - Influence of the condensation rate on the percentage of the steel surface area affected by localized corrosion

TEST #2 - T_{gas}= 45°C

A second experiment was conducted at a lower temperature (45 instead of 65°C). The primary objective was to investigate the range of test conditions (mainly temperature and water condensation rate) for which $FeCO_3$ formation and localized corrosion would be encountered in a TLC scenario.

The initial observation of the state of the slab immediately after the test showed that the extent of corrosion seemed higher on the part exposed to higher WCR. More cracks in the corrosion product layers were observed on the cooled section which is usually synonymous with higher corrosion rate. A

significant amount of iron oxide (most likely ferric oxide Fe_2O_3) was also present on the steel surface, although the concentration of O_2 in the loop was kept under 20 ppb during the test. It is thought that the oxide appeared during the slab removal process, which can take several minutes. The SEM/EDX analysis was performed on different sections of the insert but no major difference was observed due to the level of cooling. The corrosion product layer is made of a mixture of iron carbonate ($FeCO_3$), iron carbide (Fe_3C) and iron oxide (most likely Fe_2O_3), the latter being most probably formed at the end of the test during the steel insert removal procedure. Most of the steel surface was covered with $FeCO_3$, while Fe_3C could be found inside cracks in the $FeCO_3$ layer, as is commonly the case in a TLC scenario.

The surface of the steel insert was analyzed after removal of the corrosion product layer using Clarke's solution (inhibited HCl). The cooled section was clearly more affected by pitting corrosion than any other part, as was anticipated. However, the extent of TLC was somehow more severe than expected at this lower temperature. Previous testing performed with weight loss samples showed no localized corrosion and a low/moderate uniform corrosion at the top of the line at a gas temperature of 40°C [5]. Large areas of the steel slab were scanned using a 3D surface profilometer, and data on pit depth were collected (Figure 6). The effect of the condensation rate is clear, as the number of pits and the area affected by localized corrosion rate increases with the condensation rate.

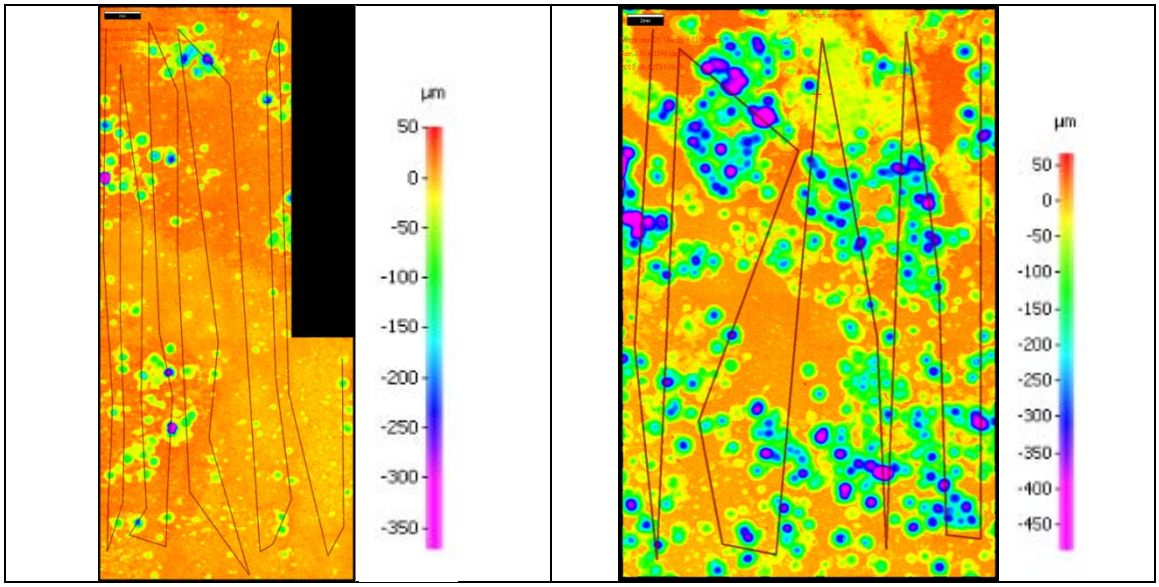

Figure 6: Test #2 - Surface profile analysis after the removal of the corrosion product layer
Left: Upstream section - Low condensation rate: 0.1 ml/m^2/s
Right: Downstream section – High condensation rate: 0.23 ml/m^2/s

TEST #3 - T_{gas}=25°C

A third experiment was conducted at an even lower temperature (25°C). The expected result was to find mostly uniform corrosion at the high range of WCRs. Preliminary observation of the state of the insert immediately after the end of the test (before removal of the corrosion product layer) shows that the corrosion product covered uniformly the surface of the steel exposed to low condensation rate. However, a very loose and poorly adherent layer covered the section of the insert exposed to higher WCR (0.1 mL/m^2/s). The layer appeared to have formed large flakes, and most of it actually fell off the steel surface as the slab was being prepared for post-processing and analysis. The "bare" steel surface underneath appeared to be uniformly corroded. It is also important to note that, for this experiment, no trace of iron oxide could be seen on the metal surface, which was mostly due to an improvement in the experimental procedures. As expected, the SEM/EDX analysis identified the corrosion product as being most likely $FeCO_3$. No other corrosion product layer could be expected in the range of pH and potential encountered in the study. Iron carbide (Fe_3C) was observed on some areas of the steel insert but this type of layer is more an indicator of high corrosion rates and exists under any experimental conditions.

Analysis of the steel surface after the removal of the corrosion product layer showed widespread localized corrosion of the middle section, exposed to a condensation rate of 0.06 mL/m^2/s. The upstream area, exposed to the lowest water condensation rate, experienced limited localized corrosion. On the other hand -- and contrary to the previous "steel insert" experiments -- no sign of localized corrosion could be found on the area of high WCR.

Large areas of the insert were scanned using a 3D surface profilometer, and data on pit depth were collected (Figure 7). As found earlier, the extent of localized corrosion clearly increased with the WCR, but only up to a certain limit (between 0.06 and 0.1 mL/m^2/s in this case). At the highest WCR tested, the steel surface was evenly corroded and no trace of localized corrosion could be found.

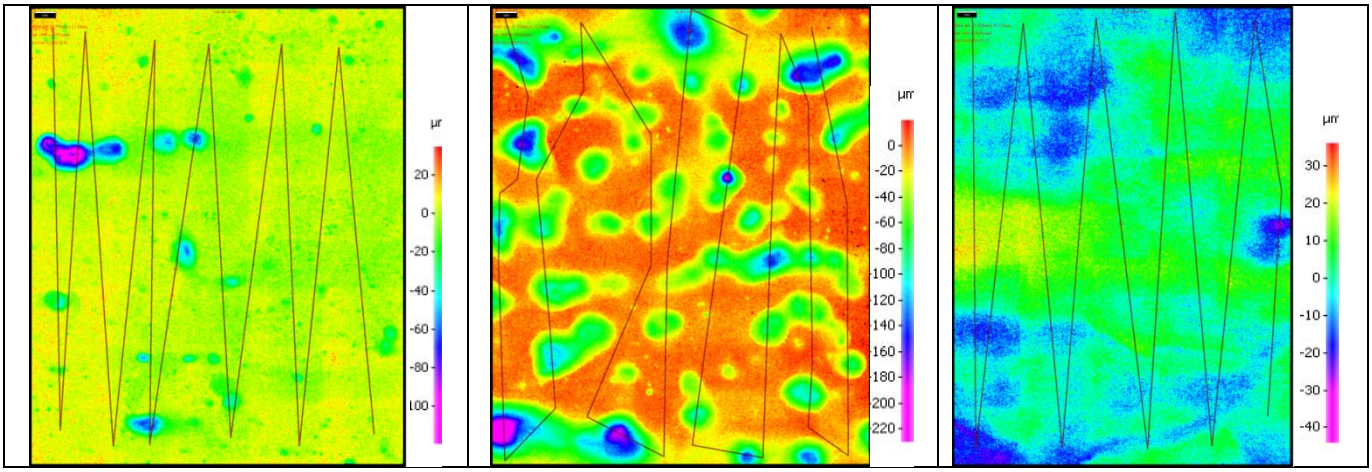

Figure 7: Test #3 - Surface profile analysis after the removal of the corrosion product layer
Left: Upstream section - Low condensation (0.038 ml/m^2/s)
Middle: Middle section - Medium condensation (0.059 ml/m^2/s)
Right: Downstream section - High condensation (0.101 ml/m^2/s)

The 3D surface profilometer data are plotted with the condensation rate in Figure 8. Localized corrosion is only sustainable in the presence of a semi-protective corrosion product layer (here $FeCO_3$), provided that this layer is adherent to the metal surface and can provide protection on some part of the steel surface. At high WCR (> 0.1 mL/m^2/s), the corrosion product layer does not adhere to the metal surface and the corrosion can consequently only be uniform in nature.

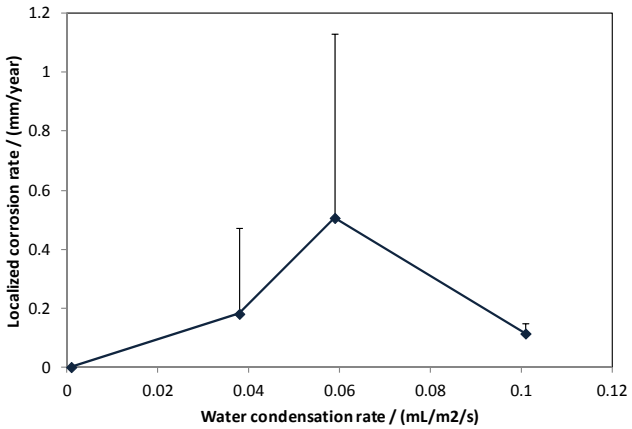

Figure 8: Test #3 - Influence of the condensation rate on the pit/mesa depth

Test #4 - Influence of the presence of acetic acid

A final experiment was performed in order to investigate the effect of a high content of organic acid on TLC, under high gas temperature and high WCR conditions. Photographs of the steel insert were taken immediately after the end of test. A thin layer of iron oxide covers most of the steel surface. The oxygen level in the loop was measured on several occasions during the test and was always below 20 ppb; it is believed that the iron oxide (most likely ferric oxide Fe_2O_3) was formed during the process of removal of the flat slab, which can take several minutes. The oxide layer was, however, very thin and superficial; it would flake off very easily, leaving behind a gray layer, expected to be iron carbonate.

The SEM/EDX analysis of the corrosion product film was performed on the different sections of the insert. There was no major variation in the film characteristics between the sections exposed to different condensation rates. The corrosion product layer is believed to be a mix of iron oxide (most likely ferric oxide Fe_2O_3), iron carbonate ($FeCO_3$) and iron carbide (Fe_3C).

The surface profile analysis was performed on the steel samples after the removal of the layer (Figure 9). The extent of the corrosion on the downstream section exposed to the highest condensation rate was impressive. The upstream section seemed much less affected, but in all cases pits were measured at similar maximum depths (800 to 1200 µm). Pits became more numerous as the condensation rate increased and tended to agglomerate together and constitute mesa attack. Large areas of the steel insert were scanned using a 3D surface profilometer, and data on pit depth were collected.

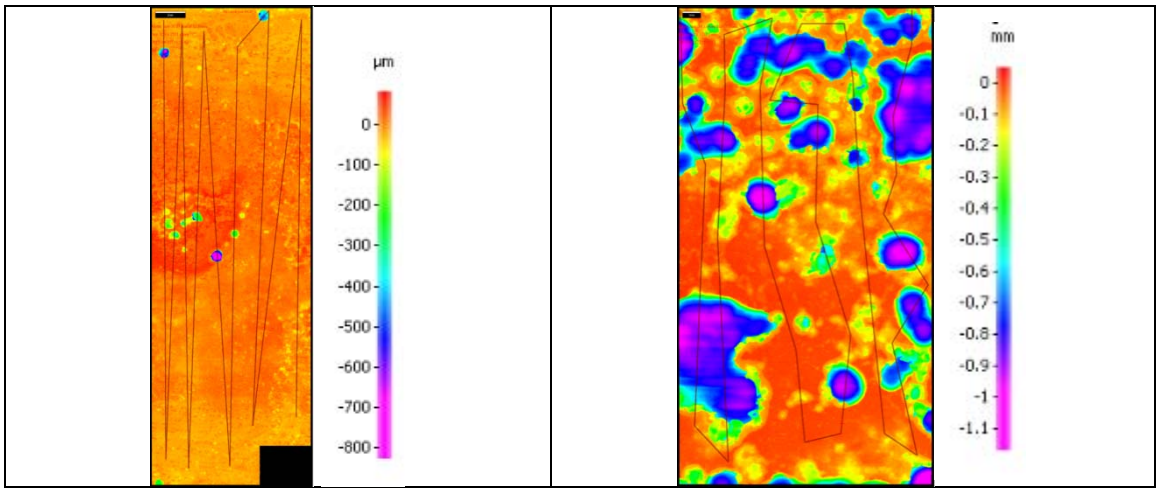

Figure 9: Test #4 - Surface profile analysis after the removal of the corrosion product layer
Left: Upstream section - Low condensation rate: 0.2 ml/m^2/s
Right: Downstream section – High condensation rate: 0.7 ml/m^2/s

Comparison between the pit depths results obtained for the short term experiments performed with weight loss samples in similar conditions showed that, as for Test #1, the localized corrosion rates (or more precisely the steel penetration rates) are about four times lower after 99 days of exposure as compared to 21 days of exposure. The presence of acetic acid does not modify the overall trend although the feature depth is significantly higher, as shown in the next section.

DISCUSSION

This section presents a summary of the experimental results obtained with the “flat slab” test section as well as some main comments of the effect of the WCR, the gas temperature and the presence of acetic acid on the extent of localized corrosion at the top of the line.

Feature characteristics could be extracted from the 3D profile analysis. An effort to collect statistical data of the pit depth distribution is also presented. The reference plane used for the profile analysis was

set to fit the top of the steel surface as much as possible. The following values were systematically computed:

- the average and maximum feature depth and corresponding localized corrosion rates,
- the average feature diameter (assuming a cylindrical shape),
- the pitting density (number of pits per unit area),
- the percentage area affected by localized corrosion.

In addition, additional statistical parameters were collected and correlated to the morphology of the localized features:

- The arithmetic mean μ calculates the average depth of features with the top steel surface as a reference. The closer the arithmetic mean is to zero, the lower is the extent of localized corrosion, in terms of depth and number of features.
- The standard deviation σ shows how much variation exists from the mean. High standard deviation indicates that the feature depth is spread out over a wide range of values.
- The root mean square (RMS) is a representation of the magnitude of the variation in pit depth over the entire surface area. A low RMS number means that the corrosion features are either shallow or very few in numbers. In the case of this study, a higher RMS number is an indication of a higher number of deeper pits.
- The skewness and kurtosis factors are used to characterize the shape of a distribution of feature depths over the entire steel surface. The tallest bar on the distribution always expresses the percentage of surface area at the “zero” or “reference” level (top surface). The skewness represents the extent to which the distribution leans to the left of this reference plan. Skewness values are consequently negative in this case since the tail of the distribution is almost always longer on the left side. A high absolute value of skewness is obtained when deep isolated pits are present on the metal surface (long and thin left tail). To the other extent, a skewness of zero is obtained when the surface is perfectly symmetrical (for example, in the case of uniform corrosion) and when there is absolutely no pit. The kurtosis is a representation of the peak characteristics (width of the peak) and tail weight. It is always a positive number that approaches zero as the distribution becomes flatter. For isolated, deep pits, the kurtosis factor will be high. Heavily pitted surfaces, where the distribution tail is thick, will have lower kurtosis factors.

- **Effect of temperature**

This section presents a comparison of the experimental results obtained at different gas temperature (65, 45 and 25°C). The tests were performed without acetic acid.

Figure 10 a) shows the effect of the water condensation on the localized corrosion rates. The water condensation rate depends on the gradient of temperature between the outside environment (steel surface) and the bulk gas. Consequently, the effect of water condensation and steel surface or gas temperature cannot be treated separately. The following comments are made:

- Low water condensation rate is often associated with high steel surface temperature (small gradient of temperature) and leads to the formation of an adherent and protective $FeCO_3$ layer. At very low gas temperature, kinetics of $FeCO_3$ formation are not favored, but super saturation is still easily reached due to the relatively low rate for condensed water renewal. $FeCO_3$ can precipitate and pits can initiate but do not seem to progress with time.
- High water condensation rate is often associated with lower steel surface temperature (larger gradient of temperature). Two sub-cases are then identified:
    - If a partially adherent/protective $FeCO_3$ layer forms (due to moderate steel temperature), localized corrosion is initiated and can be very severe.
    - If the steel temperature is too low to form an adherent corrosion product layer, localized corrosion cannot be initiated and the corrosion is uniform.
- At lower gas temperature, high water condensation rates are difficult to achieve, as the water vapor pressure is lower. However, for a fixed water condensation rate, the average and maximum localized corrosion rates are only marginally higher at higher temperature.

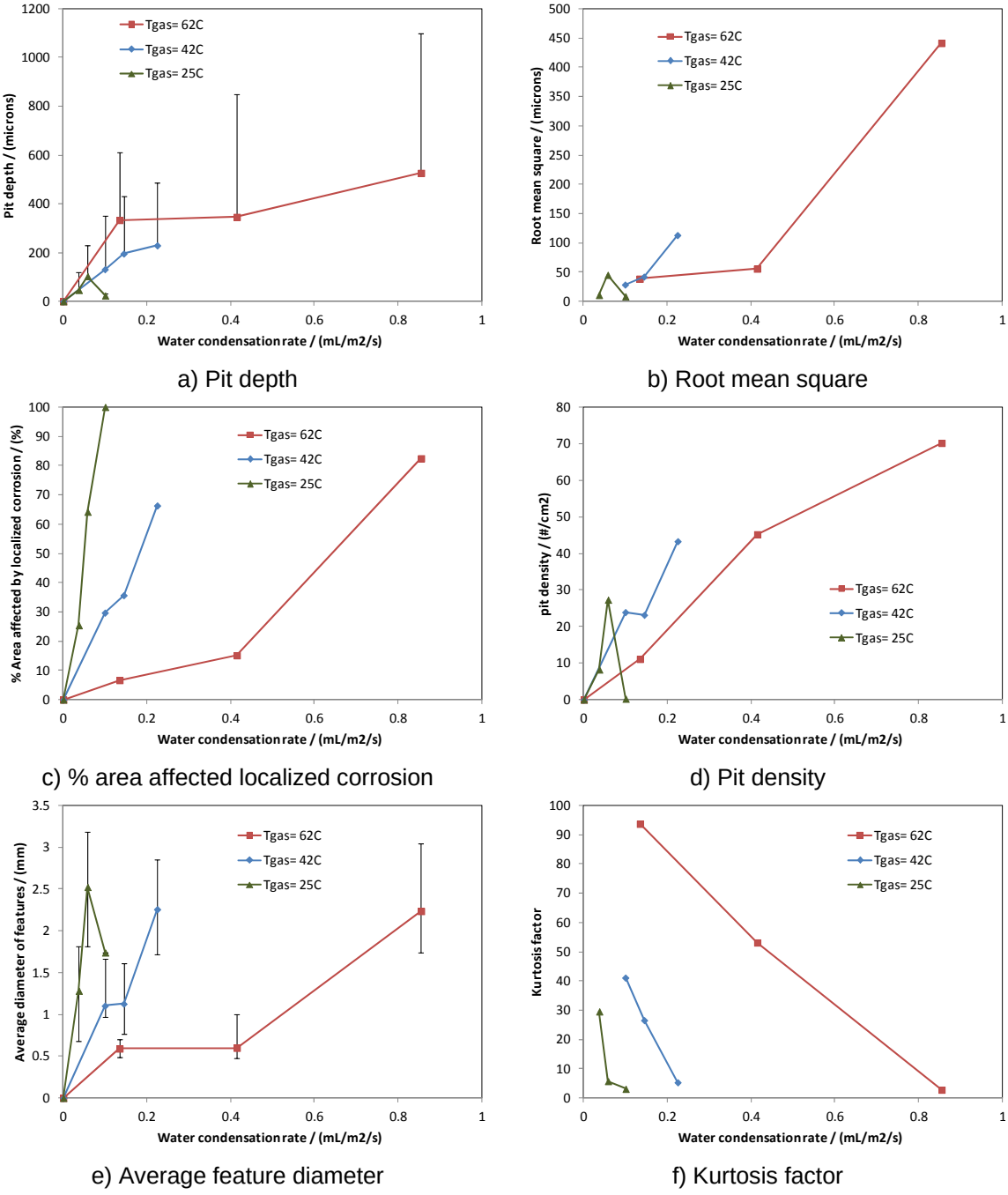

Figure 10: Influence of the gas temperature and the water condensation rate

Summary of results

The main influence of the gas temperature is seen in the percentage area affected by localized corrosion, which increases very rapidly with water condensation rate at lower temperature (Figure 10 c)). The corrosion attack switches from localized to uniform over a small variation of condensation rates. This is reflected by an increase in $FeCO_3$ solubility at low temperature and the difficulty to form an adherent and protective corrosion product layer. The maximum feature diameter is similar in all conditions tested but the features will be correspondingly deeper at higher temperature (Figure 10 a) and e)).There is also a logically greater variation in the feature depth distribution at higher temperature (Figure 10 d)) since the features are often deeper and more isolated than at lower temperature.

- **Influence of the presence of acetic acid**

This section presents a comparison of the experimental results obtained at different acetic acid concentrations (0 and 1000ppm). Statistical parameters are consistent with a wide variation in corrosion feature depth, especially at high water condensation rates (Figure 11 b)) and the presence of deep but isolated pits at lower WCR (Figure 11 f)). The main effect of the presence of acetic acid is seen at high WCR on the average feature diameter and the percentage area of the steel surface affected by localized corrosion (Figure 11 c) and e)). Since the solution is more aggressive, pits seem to cluster more easily and mesa type attack is more wide spread. The decrease in pitting density with acetic acid (Figure 11 d)) is due to the increase in feature size.

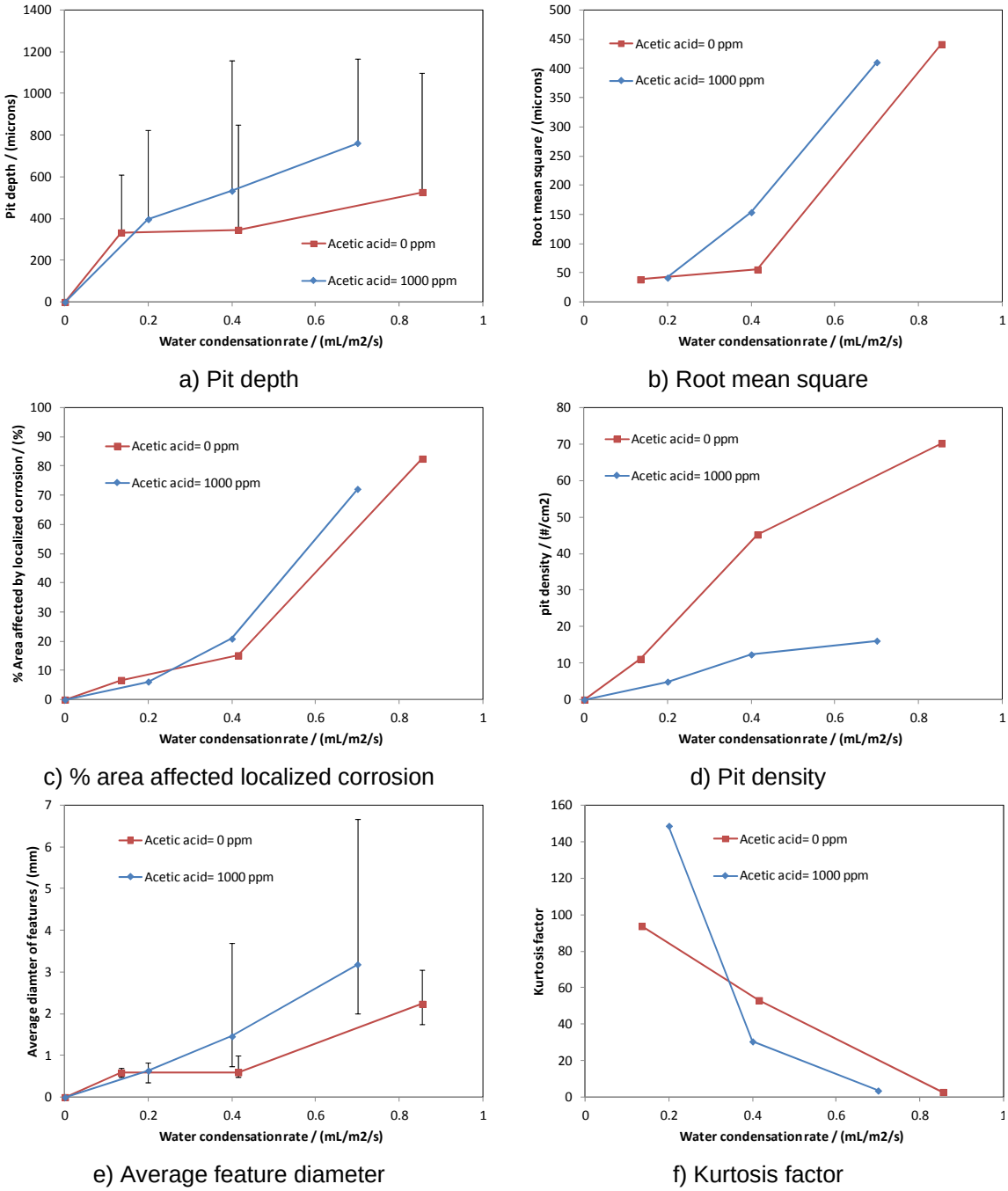

a) Pit depth

b) Root mean square

c) % area affected localized corrosion

d) Pit density

e) Average feature diameter

f) Kurtosis factor

Figure 11: Influence of the acetic acid concentration and the water condensation rate Summary of results

The presence of 1000 ppm of undissociated acetic acid did not completely change the picture as compared with the baseline test. However, the extent of the corrosion attack was more severe due to the presence of the acetic acid. This is expected since the presence of an additional acid in solution decreases the pH of the condensed water, acts as a buffer (with related acetate) with regard to hydrogen ions and increases the solubility of $FeCO_3$. Average and maximum pits depths are also consequently higher in the presence of organic acid.

CONCLUSIONS

A new experimental setup (carbon steel inserts in flat slab) was developed to improve the quality of the experimental data. The new set of experiments was successful in simulating TLC without obvious edge effects and in capturing the effect of the condensation rate. Localized corrosion could be very clearly observed on the steel surface and correlated to the condensation rate and the gas temperature.

- Pitting/mesa corrosion is strongly related to the level of condensation applied to the steel section.
- On the thermally insulated areas, localized corrosion is marginally observed but does not grow with time after the first months of exposure.
- On the cooled section, pits still seem to be growing in depth with time and also form clusters.
- In the presence of undissociated acetic acid, the extent of the corrosion attack was much more severe compared to previous results obtained without acetic acid. Especially, the condensation rate did not seem to have a strong effect on the maximum depth of the corrosion features.
- These observations are in agreement with field observation of TLC.

REFERENCES

1. Y. Gunaltun, D. Supriyataman and A. Jumakludin, “Top of the line corrosion in multiphase gas line. A case history”, in *Proc. Corrosion*, Houston, TX, 1999, paper no. 36.
2. S. Olsen, A. Dugstad, “Corrosion under dewing conditions”, in *Proc. Corrosion*, Houston, TX, 1991, paper. 472.
3. B.F.M. Pots, E.L.J.A. Hendriksen, “CO_2 corrosion under scaling conditions – The special case of top-of-the-line corrosion in wet gas pipelines”, in *Proc. Corrosion*, Houston, TX, 2000, paper. 31.
4. F. Vitse, “Experimental and theoretical study of the phenomena of corrosion by carbon dioxide under dewing conditions at the top of a horizontal pipeline in presence of a non-condensable gas”, PhD dissertation, Russ College of Eng., Dept. of Chem. Eng., Ohio Univ., Athens, OH, 2002.
5. M. Singer, D. Hinkson, Z. Zhang, H. Wang and S. Nesic, “CO_2 top of the line corrosion in presence of acetic acid - a parametric study”, in *Proc. Corrosion*, Atlanta, GA, 2009, paper. 9292.
6. C. Mendez, M. Singer, A. Camacho, S. Hernandez and S. Nesic, “Effect of acetic acid, pH and MEG on CO_2 top of the line corrosion”, in *Proc. Corrosion*, Houston, TX, 2005, paper. 5278.
7. R. Nyborg and A. Dugstad, “Top of the line corrosion and water condensation rates in wet gas pipelines”, in *Proc. Corrosion*, Nashville, TN, 2007, paper. 7555.
8. Z. Zhang, D. Hinkson, M. Singer, H. Wang and S. Nesic, “A mechanistic model for Top of the line corrosion”, *Corrosion*, vol. 63, no. 11, pp. 1051-1062, Nov. 2007.
9. A. Rotimi, R.A. Ojifinni, C. Li, “A parametric study of sweet top of the line corrosion in wet gas pipelines”, in *Proc. Corrosion*, Houston, TX, 2011, paper. 11331.
10. M. Thammachart, Y. Gunaltun and S. Punpruk, “The use of inspection results for the evaluation of batch treatment efficiency and the remaining life of the pipelines subjected to top of line corrosion”, in *Proc. Corrosion*, New Orleans, LA, 2008, paper. 8471.
11. J. Amri, E. Gulbrandsen and R.P. Nogueira, “The effect of acetic acid on the pit propagation in CO_2 corrosion of carbon steel”, *Electrochemistry Communications*, vol. 10, pp. 200–203, 2008.
12. M. Singer, “Study and Modeling of the Localized Nature of Top of the Line Corrosion”, PhD dissertation, Russ College of Eng., Dept. of Chem. Eng., Ohio Univ., Athens, OH, 2013.
13. Y. Gunaltun and D. Larrey, “Correlation of cases of top of the line corrosion with calculated water condensation rates”, in *Proc. Corrosion*, Houston, TX, 2000, paper. 71.